12-5-2016

Efficiency from Added Control and Root Cut Out in Infinite Blade Rotorcraft

Brian D. Mincks
Washington University in St. Louis

David Peters
Washington University in St. Louis

Efficiency from Added Control and Root Cut Out in Infinite Blade Rotorcraft

Brian Mincks
b.d.mincks@wustl.edu
Graduate Student
Washington University in St. Louis

Dr. David A. Peters
dap@wustl.edu
McDonnell Douglas Professor of Engineering

JunSoo Hong
jh25@wustl.edu
PhD Student

ABSTRACT

A dynamic inflow based induced power model for a lifting rotor with an infinite number of blades is analyzed to reveal efficiency of a rotorcraft in forward flight. The model starts from first principals to relate the acceleration potential of an actuator disk to pressure on the lifting blade. Peters and He Ref [3] note that this model provides "overall good correlation with recent measurement data" (xix). This model is extended with the addition of harmonic control, radial control, and root cut out (rco). The addition of these three factors reveal ways to approach the minimum induced power as predicted by Glauert.

NOTATION

$[\bar{A}]$	effect of control input
$\{C\}$	rotor loading constraints
$\{\bar{C}\}$	normalized loading constraints, $\{C\}/C_T$
C_L	roll moment coefficient
C_M	pitch moment coefficient
C_P	induced power coefficient
C_T	thrust coefficient
D	maximum order of blade radial twist control polynomial
$[\bar{D}]$	matrix relating pressure states to rotor loads
H	maximum harmonic of blade pitch control
$[I]$	identity matrix
$[\bar{L}^e]$	matrix relating pressure state to inflow state
$[\bar{L}^e]_{sym}$	symmetric part of $[\bar{L}^e]$
ΔP	non-dimensional pressure difference
$\mathrm{P}_n^m(\nu)$	normalized Legendre function
$[\bar{P}]$	matrix relating pressure states to control variables
R	blade radius
rco	root cutout, fraction of blade radius
$\bar{r}$	non-dimensional radial position
t	time
$[U]$	flipping matrix
V	$\sqrt{\mu^2+\lambda^2}$
$\omega(\bar{r},\psi)$	non-dimensional induced flow
α_s	nose up shaft angle
$\{\gamma\}$	inflow state
$\theta(\bar{r},\psi)$	blade pitch angle
$\{\bar{\theta}\}$	rotor control
λ	inflow due to shaft tilt $= -\mu\alpha$
$\{\bar{\Lambda}\}$	Lagrange multiplier
μ	advance ratio $= V\sin(\chi)$
ν	ellipsoidal coordinate
ρ	air density
σ	solidity
$\{\bar{\tau}\}$	pressure states
$\phi_n^m(\bar{r})$	inflow expansion function
ψ	azimuth angle

INTRODUCTION

Harris, ref. [1], explains that a rotorcraft in high speed, forward flight uses six to eight times Glauert's ideal minimum induced power. This paper addresses these inefficiencies using a method developed by Peters and He, Refs. [2], [3], [4], called dynamic inflow theory. Dynamic inflow applies potential flow to a rotorcraft lifting blade. The theory is more robust and accurate than uniform inflow theories yet computationally faster than modern vortex based computational fluid dynamic technics. Therefore, it can account for the radial and azimuthal nonuniformities in the induced velocity inflow distribution that contribute to inefficiency while leaving run time in the reasonable domain. Throughout the development of dynamic inflow theory, Ormiston Refs. [2-5] shows that the inefficiency of a rotorcraft is due to the inability of the blade to trim through non-uniform inflow. In further developments, Ormiston found an infinite power peak at the critical advance ratio, while Hall and Hall Ref. [6] found a finite peak using a vortex lattice method. After the work of Hall and Hall, Ormiston suggests that the induced power can be directly obtained through analytical derivation. Peters and File Refs [7-8] explored this claim with the use of a quadratic optimization to find the induced power. Their results

mimic that of Hall and Hall in that they find a finite peak in induced power around the advance ratio 0.8.
In this paper, the work of Peters and File has been extended to include added harmonic control, added radial control, and root cut-out. I assume a rotorcraft with an infinite amount of control will generate the induced power as predicted by Glauert and I hypothesize that there exists a minimum finite amount of control paired with root cut out that will yield the same result.

THEORY

Peters and He model inflow and pressure distribution across the rotor disk with inflow and pressure states $\{\bar{\gamma}\}$ and $\{\bar{\tau}\}$ respectively Ref [9]. They found inflow and pressure difference to be:

$$(\mathbf{1}) \qquad \omega(\bar{r},\psi) = \sum_{r=-\infty}^{\infty} \sum_{j=|r|+1,\ |r|+3\ldots}^{\infty} \phi_j^r(\bar{r})\gamma_j^r e^{ir\psi}$$

$$(\mathbf{2}) \quad \Delta P(\bar{r},\psi) = \sum_{m=-\infty}^{+\infty} \sum_{n=|m|+1,|m|+3,\ldots}^{+\infty} \bar{P}_n^m(\nu)\bar{\tau}_n^m e^{im\psi}$$

where

$$(\mathbf{3}) \qquad \nu = \sqrt{1-\bar{r}^2}$$

Ormiston develops the inflow-pressure relationship, Ref [4]. In complex form, it is:

$$(1) \qquad \{\gamma_n^m\} = \left({}^{1}/_{2V}\right)\cdot[\bar{L}^e]\{\bar{\tau}_n^m\}$$

The induced power is calculated using Equation 2, to multiply pressure by the rotor disk area.

$$(2) \qquad C_P = \frac{1}{\pi}\int_0^{2\pi}\int_{rco}^{1} w\Delta P\cdot\bar{r}\cdot d\bar{r}d\psi$$

Hong Ref [10] expands this derivation further to obtain Equations 6 and 7 by substituting Eqs. (1) and (2) into Eq. (5) and solving the double integral

$$(3) \qquad C_P = 2\sum_m \sum_n \{\bar{\tau}_n^{-m}\}^T\{\gamma_n^m\}$$

He further substitutes Equation 4 to obtain

$$(4) \qquad \begin{aligned} C_P &= \left({}^{1}/_{V}\right)\sum_m \sum_n \{\bar{\tau}_n^{-m}\}^T[\bar{L}^e]\{\bar{\tau}_n^m\} \\ &= \left({}^{1}/_{V}\right)\{\bar{\tau}\}^T[U][\bar{L}^e]\{\bar{\tau}\} \end{aligned}$$

With the skew angle close to 90° a small angle approximation reveals that the mass flow, V, is approximately equal to the advance ratio. Therefore, induced power is a function of pressure states.

Hong extends the induced power derivation to specify thrust, roll, and pitch.

$$(5) \qquad \begin{aligned} C_T &= {}^{1}/_{\pi}\int_0^{2\pi}\int_0^{1} \Delta P\cdot\bar{r}\cdot d\bar{r}\cdot d\psi \\ C_L &= -{}^{1}/_{\pi}\int_0^{2\pi}\int_0^{1} \Delta P\cdot\left(\bar{r}\cdot\sin(\psi)\right)\cdot\bar{r}\cdot d\bar{r}\cdot d\psi \\ C_M &= -{}^{1}/_{\pi}\int_0^{2\pi}\int_0^{1} \Delta P\cdot\left(\bar{r}\cdot\cos(\psi)\right)\bar{r}\cdot d\bar{r}\cdot d\psi \end{aligned}$$

To simplify he uses:

$$(6) \qquad \{C\} = \begin{bmatrix} 0 & {}^{2}/_{\sqrt{3}} & 0 \\ i\sqrt{{}^{2}/_{15}} & 0 & -i\sqrt{{}^{2}/_{15}} \\ -\sqrt{{}^{2}/_{15}} & 0 & -\sqrt{{}^{2}/_{15}} \end{bmatrix}\{\bar{\tau}\}$$

or simply

$$(7) \qquad \{C\} = [\bar{D}]\{\bar{\tau}\}$$

where

$$(11) \qquad [\bar{D}] = \begin{bmatrix} 0 & {}^{2}/_{\sqrt{3}} & 0 \\ i\sqrt{{}^{2}/_{15}} & 0 & -i\sqrt{{}^{2}/_{15}} \\ -\sqrt{{}^{2}/_{15}} & 0 & -\sqrt{{}^{2}/_{15}} \end{bmatrix}$$

To factor in the effect of added control, Hong continues deriving to make equation 10 a function of control. This control can be modeled with the pitch angle:

$$(12) \qquad \theta(\bar{r},\psi) = \sum_{h=-\mathrm{H}}^{+H} \sum_{d=0}^{D} \bar{r}^d\bar{\theta}_d^h e^{ih\psi}$$

where $H \geq 1$ and $D \geq 0$. He uses this equation to put the control into the vector form:

$$\{\bar{\theta}\} = \begin{Bmatrix} \vdots \\ \bar{\theta}_d^h \\ \vdots \\ \alpha_s \end{Bmatrix} \quad (13)$$

He finally finds the new form of equation 10.

$$\{C\} = [\bar{D}][\bar{P}]\{\bar{\theta}\} \quad (14)$$

where $[\bar{P}]$ relates the control variables to pressure states. This equates equations 10 and 14 meaning

$$\{\bar{\tau}\} = [\bar{P}]\{\bar{\theta}\} \quad (15)$$

Using this, equation 7 becomes

$$C_P = \left({}^{1}/_{V}\right)\{\bar{\theta}\}^T[\bar{P}]^T\{\bar{\theta}\}^T[U][\bar{L}^e][\bar{P}]\{\bar{\theta}\} \quad (16)$$

After optimization using Lagrange multipliers, Hong finds the normalized induced power to be:

$$\left(\frac{C_P}{{C_T}^2}\right) = \left({}^{1}/_{V}\right)\{\bar{C}\}^T[\bar{Q}]^{-1}\{\bar{C}\} \quad (17)$$

Here, $\left({}^{1}/_{V}\right)$, $[\bar{Q}]^{-1}$, and $\{\bar{C}\}$ are the Lagrange multiplier.

$$\{\bar{\Lambda}\} = \left({}^{1}/_{V}\right)[Q]^{-1}\{C\} \quad (18)$$

and

$$[\bar{Q}] = \left([\bar{D}][\bar{P}]\left([\bar{P}]^T[U][\bar{L}^e]_{sym}[\bar{P}]\right)^{-1}[\bar{P}]^T[\bar{D}]^T\right) \quad (19)$$

Equation (17) is used throughout the entirety of this paper as it is compared to the minimum normalized induced power predicted by Glauert:

$$\left(\frac{C_P}{{C_T}^2}\right)_{ideal} = \frac{1}{2\mu} \quad (20)$$

TOOLS

All calculations were done using MATLAB.

ALGORITHMS

The inflow expansion function needs to be used for each unique set of parameters *H, D, rco*, and blade element size in order to calculate the matrix that relates pressure states to inflow states. This matrix is needed to calculate the normalized induced power. The expansion function takes on the order of thousands of seconds to calculate for our project because our blade element cut size is 100. The math works out so that adding one more increment of harmonic control will add more rows to the matrix. However, when more harmonic control is added it works out that everything except for the new rows added is the same as the matrix with one less increment of harmonic control. Consider the simplified example:

H = n	*H = n + 1*
a	*a*
b	*b*
not calculated	*c*

I noticed this trend and modified the calculation. If the program has already calculated the matrix with one less increment of harmonic control, it simply plugs in values from a previously saved matrix and skips to the calculations it hasn't done. This improvement decreased run time on the order of two orders of magnitude in extreme cases. Once I noticed this trend, I searched for more redundant calculations to expedite the run time for future works. I found another redundancy in the matrix that relates pressures states to inflow states: $[\bar{L}^e]$. In this calculation, more harmonic control adds more calculations, however, the location of the redundancy in the matrix was much different. These matrices are square and the redundancies occur in the center. Consider the simplified example where *X* represents a new calculation.

H = n

a	*b*
c	*d*

H = n + 1

X	*X*	*X*	*X*
X	*a*	*b*	*X*
X	*c*	*d*	*X*
X	*X*	*X*	*X*

Again, I modified the calculations so that nothing was calculated twice. This improved run time in extreme cases by a factor of 12.

EFFECTS OF ADDED CONTROL

We use equations (17) and (20) to investigate how much power will be saved at all advance ratios.

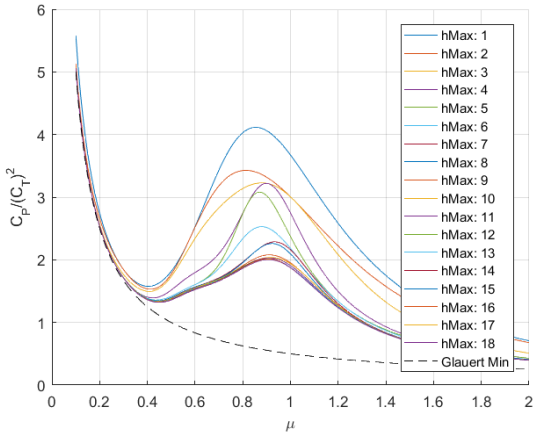

***Figure 1**: Normalized induced power vs. advance ratio with fixed D = 0.*

At first, I experimented with only adding harmonic control to fixed radial control as seen in Figure 1. I found the trend of diminishing returns that we predicted at the start of the project. As it's seen here, when the harmonic control approaches infinity added efficiency is zero. However, this convergence does not occur at Glauert's minimum so I decided to repeat this process for different values of radial control to see where the efficiency converged.

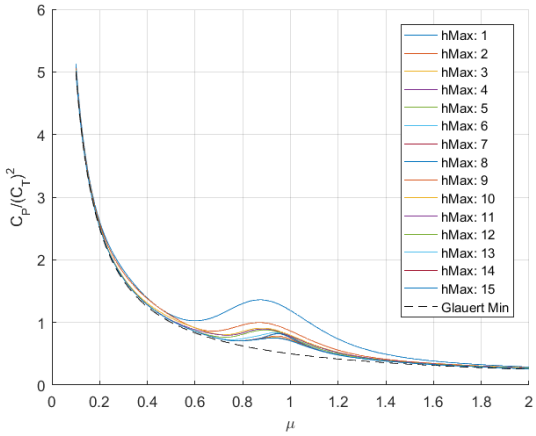

***Figure 2**: Normalized induced power vs. advance ratio with fixed D = 1.*

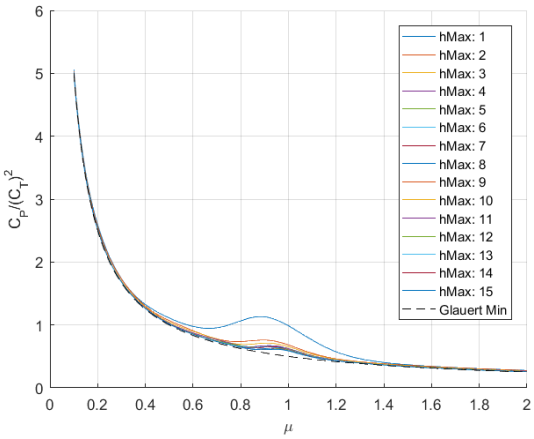

***Figure 3**: Normalized induced power vs. advance ratio with fixed D = 2.*

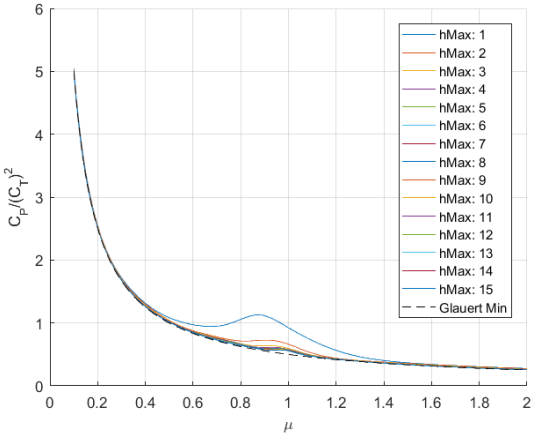

***Figure 4**: Normalized induced power vs. advance ratio with fixed D = 3.*

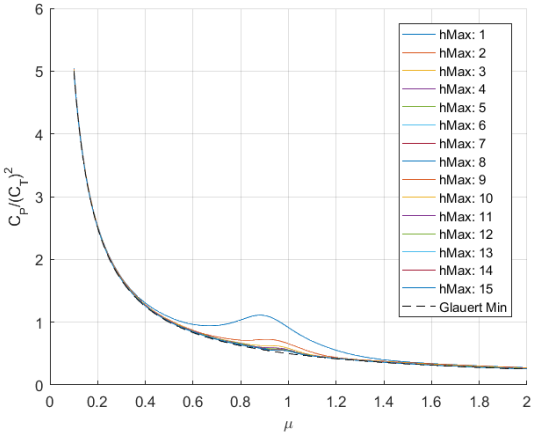

***Figure 5**: Normalized induced power vs. advance ratio with fixed D = 4.*

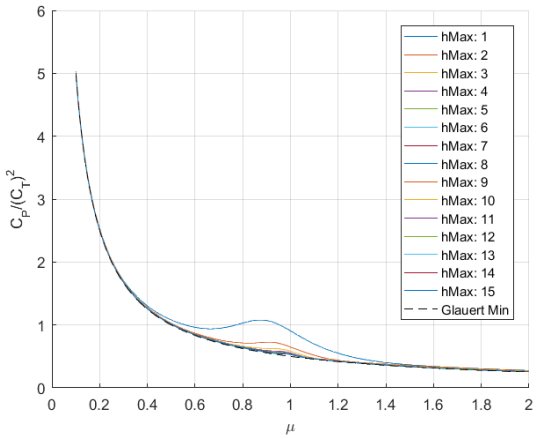

***Figure 6**: Normalized induced power vs. advance ratio with fixed D = 5.*

I developed an algorithm that calculated the relative error, *E*, between induced power curves at fixed radial control and varying harmonic control. When comparing a curve of control $H = n$ to a curve with control $H = n + 1$, I called three different relative errors converged: $E = 1$, $E = .5$, $E = .1$. The *H* value at which maximum efficiency can be achieved with fixed *D* is seen in Figure 7.

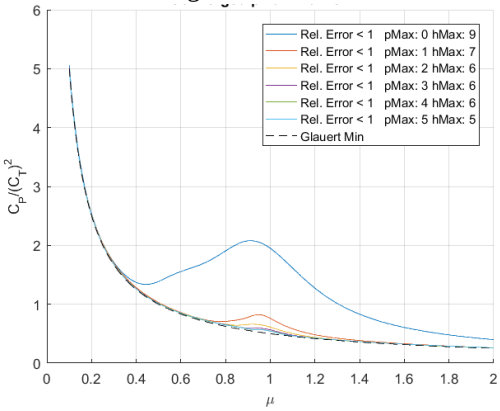

***Figure 7**: Converged (E < 1%) normalized induced power vs. advance ratio for varying H.*

This figure revealed another trend: as *D* increases, it requires less *H* for the induced power curve to converge. This trend was investigated to reveal the relationship needed between *H* and *D* to achieve maximum efficiency at a fixed *D*. This effectively shows when additional *H* is useless at a fixed *D*. The results are seen in Figure 8 for varying amounts of desired convergence.

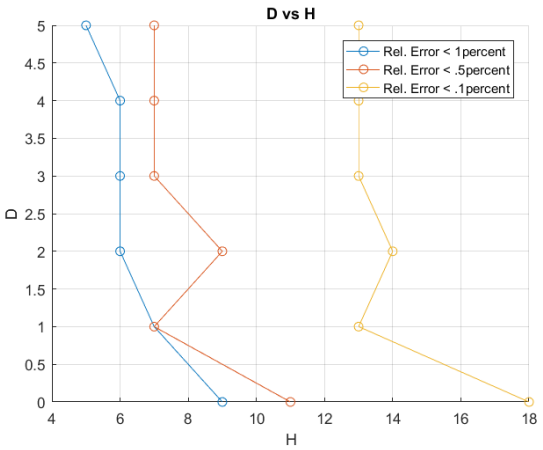

***Figure 8**: H with maximum efficiency at a fixed D with varying convergence.*

With the ability to find where *H* converges for a fixed *D*, we used equation 11 to investigate the induced power at every azimuthal angle and radial position on the blade.

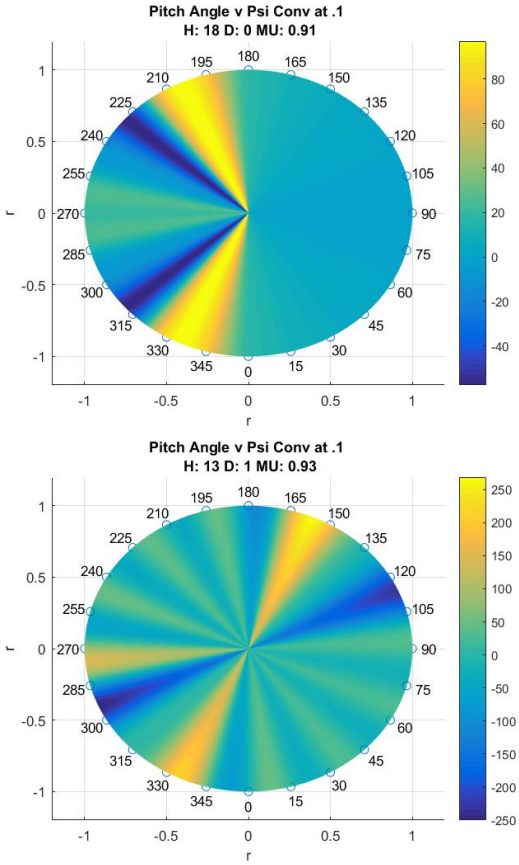

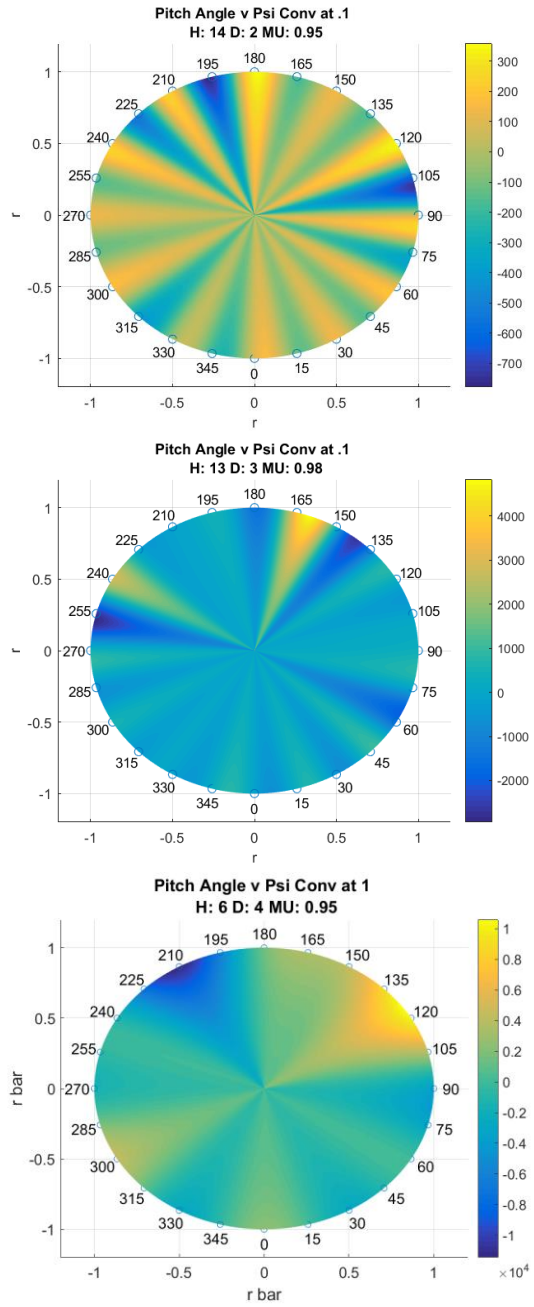

***Figure 9**: Top view of pitch angle*

Notice that $D = 5$ is missing from these plots. This wasn't calculated because there is no critical advance ratio when H converges for this much of D. This paired with Figure 7 shows that a finite amount of control can effectively produce the Glauert's minimum induced power.

ROOT CUT OUT

The concept of root cut out is simply to have an infinitesimally small nonlifting bade that connects a lifting blade to the rotation mast at some distance.

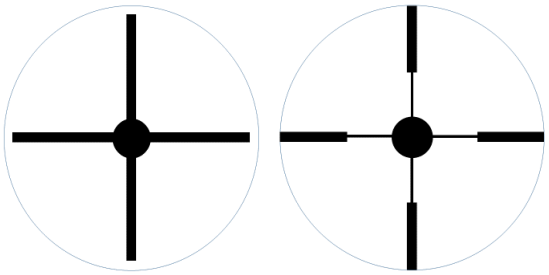

***Figure 10**: Conventional blade (left) and root cut out blade (right).*

Hong finds that induced power can be reduced by *rco*. He proved this mathematically by using a modified version of equation 15 in the previously described methods.

$$\{\bar{\tau}\} = \frac{\sigma a}{4} \cdot \left[[\bar{A}]\{\bar{\theta}\}\right] \tag{18}$$

where

$$[\bar{A}] = \begin{pmatrix} \left[\int_{rco}^{1} \left[\bar{r}^{(2+p)}\right]\left[\phi_n^m\right] \cdot dr\right] \cdot e^{i(h-m)\bar{t}} \\ + (i) \cdot \mu \cdot \left[\int_{rco}^{1} \bar{r}^{(1+p)}\left[\phi_n^m\right] \cdot dr\right]\left[-e^{i(h-m+1)\bar{t}} + e^{i(h-m-1)\bar{t}}\right] \\ + \left(-\frac{1}{4}\right) \cdot \mu^2 \cdot \left[\int_{rco}^{1} \bar{r}^{p}\left[\phi_n^m\right] \cdot dr\right] \cdot \left[e^{i(h-m+2)\bar{t}} - 2e^{i(h-m)\bar{t}} + e^{i(h-m-2)\bar{t}}\right] \end{pmatrix} \tag{19}$$

As seen in Figure 11, a fair amount of pressure difference occurs in the region near the rotaion mast. This causes a spike in induced power. Therefore, if we could simply avoid this region all together with an *rco* blade, we could improve efficiency. Notice from the figure below that *rco* is a normalized radius and therefore its value is simply the percent of the blade radius that is cut out from the middle outward.

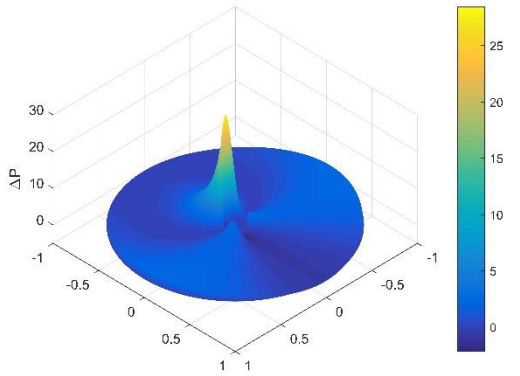

***Figure 11**: Pressure distributed across the disk with advance ratio = .9. Hong Ref. [10].*

Hong notes that at moderate amount of root cut out causes the inflow velocity distribution to become more uniform.

Initial calculations revealed two trends that needed investigation. As seen below, the optimal *rco* is dependent on the advance ratio. Also, in some situations, there is more than one optimal *rco*.

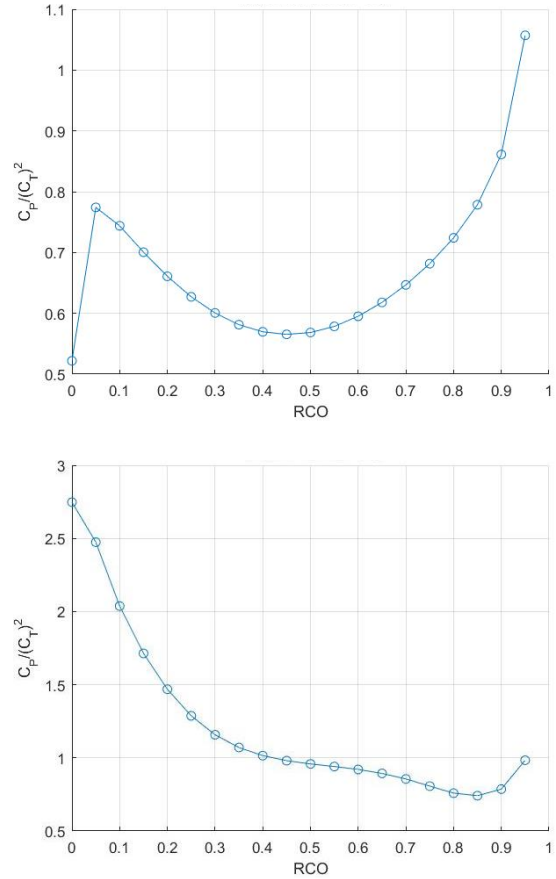

***Figure 12**: C_p vs rco H = 4 D = 0. The top plot has advance ratio of 1.8 and the bottom has advance ratio of 1.*

To investigate these trends, I developed an algorithm that both found the optimal *rco* for each advance ratio while looking for two minimums. This algorithm turned out to have the longest run time of any part of the project. To make this more efficient, I extended the algorithm to have a broad initial search for the most efficient *rco*. It would start by calculating all the *rco* values in our domain in increments of .05. It would then up the precision of the *rco* search by an order of magnitude and restrict its domain to areas that were around the most efficient or areas where a second minimum was detected. It effectively zoomed in until the optimal rco was calculated to four significant digits. After this algorithm was perfected, it produced the exact same results as the conventional method where everything was calculated, but it cut run time down by two orders of magnitude. Figure 13 shows an example of the most complicated case that the algorithm had to tackle. There are two situations where two minimums are found.

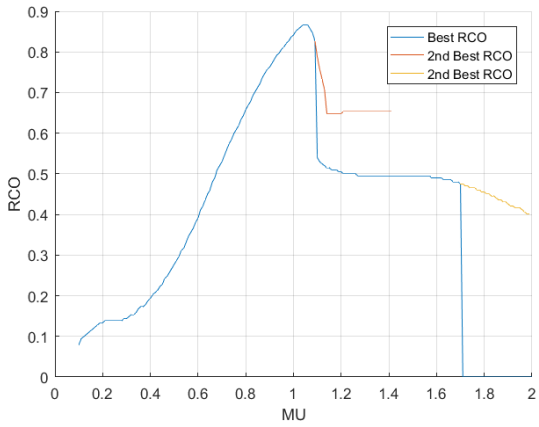

***Figure 13**: Most efficient rco for all advance ratios. H = 4 D = 0.*

We moved on to compare the normalized induced power to Glauert's minimum when the *rco* was most efficient for all advance ratios with varying amounts of control. Figure 13 shows efficiency for arbitrary amounts of control. We included data for *rco = 0* from previous analysis to derive how much more efficiency is gained with *rco*.

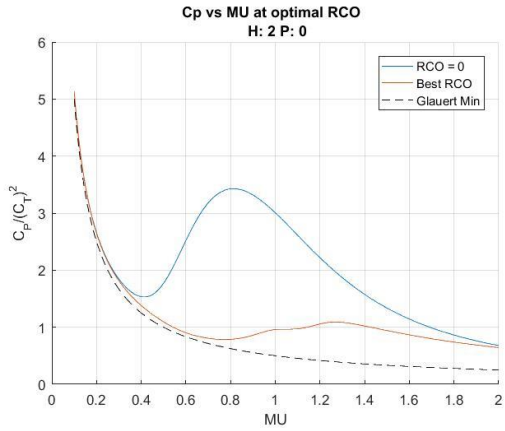

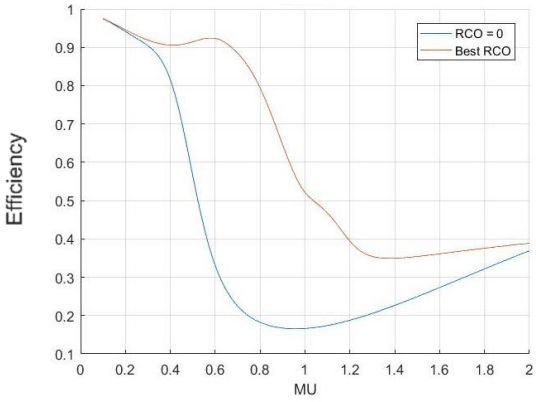

***Figure 13**: H = 2 P = 0. Normalized induced power at all advance ratios when the blade is at the optimal rco (top). The bottom shows the same information as a percent efficiency.*

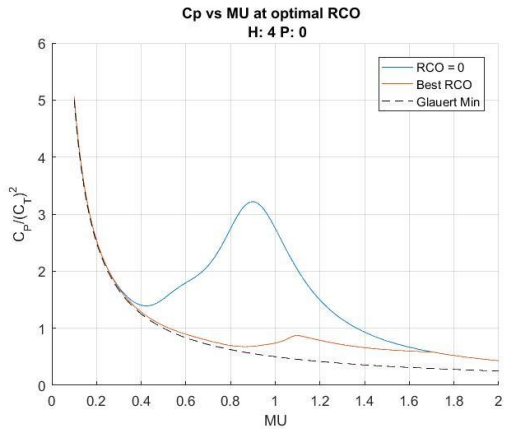

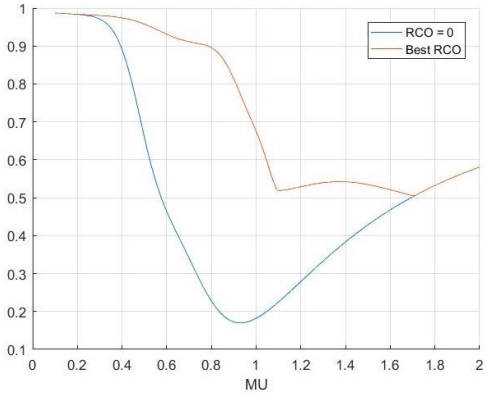

***Figure 14**: H = 4 P = 0. Normalized induced power at all advance ratios when the blade is at the optimal rco (top). The bottom shows the same information as a percent efficiency*

.

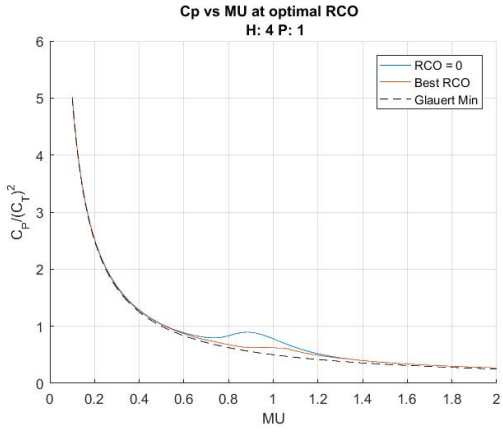

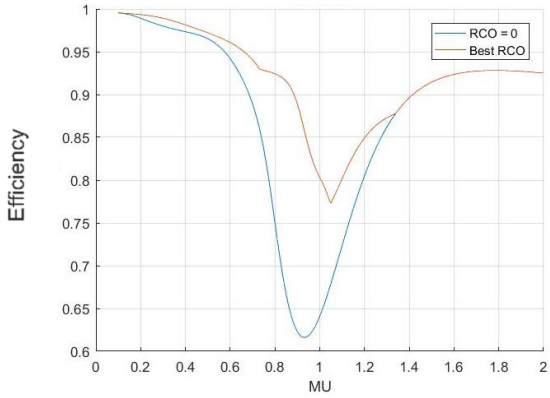

***Figure 15**: H = 4 P = 1. Normalized induced power at all advance ratios when the blade is at the optimal rco (top). The bottom shows the same information as a percent efficiency.*

As Figures 13-15 show, *rco* drastically improves efficiency in the domain of the critical advance ratio. With the ability to determine when additional power

becomes useless and the ability to find the most efficient *rco* at all advance ratios, I decided to put everything together to see just how efficient a rotorcraft would become if I could apply any conditions I wanted. I pulled the strongest control converged at $E < .1\%$ to find the results of Figure 16.

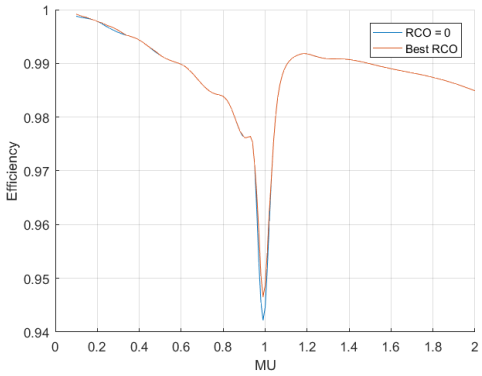

.

Figure 16: *Efficiency H = 13, D = 5, and optimal rco at all advance ratios*

As seen, if this research can be taken to its extreme, a rotorcraft can attain above 94% efficiency at all advance ratios.

CONCLUSION

This research shows that a finite amount of control can be added to a rotorcraft and provide approximately all the efficiencies of that of infinite control. It shows where the addition of harmonic control becomes useless for each increment of radial control. This will be useful as a road map for research and development of future rotorcraft. Furthermore, this research shows that for a certain amount of radial control, the convergence point of added harmonic control is Glauert's minimum induced power. I further continued the study of efficiency by investigating root cut out to show efficiency could be gained when additional control is minimal and when additional control is at an extreme.

Future studies will include additional aerodynamic phenomenon that contribute to induced power such as inflow feedback, reverse flow, and wake generated by a finite number of blades.

ACKNOWLEDGEMENTS

I would like to thank Dr. Dave Peters for allowing me to be a part of this project. I also want to thank Sean Hong for his time spent answering my endless barrage of questions and emails.

REFERENCES

1. Glauert, H., "A General Theory of the Autogyro," R&M No. 1111, Aeronautical Research Council of Great Britain, March 1927.

2. File, Chad, Peters, David A., and Ormiston, Robert A., "Optimum Rotor Performance with Realistic Constraints by Finite-State Induced Flow Methods," Proceedings of the 67th Annual National Forum of the American Helicopter Society, Virginia Beach, Virginia, May 3-5, 2011.

3. File, Chad L, *Optimization of Induced-Power from Dynamic Inflow Theory*, Ph.D. Dissertation, Washington University in St. Louis, May 2013.

4. He, Cheng Jian, *Development and Applications of a Generalized Dynamic Wake Theory for Lifting Rotors*, Ph.D. Dissertation, Georgia Institute of Technology, August 1989.

5. Harris, Franklin D., "Rotary Wing Aerodynamics Historical Perspectives and Important Issues," paper presented at the American Helicopter Society Southwest Region National Specialists' Meeting on Aerodynamics and Aeroacoustics, Arlington, TX, February 25-27, 1987.

6. Ormiston, Robert A., "Helicopter Rotor Induced Power," Proceedings of the AHS International 60th Annual Forum and Technology Display, Baltimore, MD, June 8-10, 2004.

7. Ormiston, Robert A., "Further Investigations of Helicopter Rotor Induced Power," Proceedings of the AHS International 61st Annual Forum and Technology Display, Grapevine, Texas, June 1-3, 2005.

8. Ormiston, Robert A., "A New Formulation for Lifting Rotor Performance Including Comparison with Full-Scale Data," Proceedings of the AHS International 64st Annual Forum and Technology Display, Montreal, Quebec, Canada, April 29 - May 1, 2008.

9. Garcia-Duffy, Cristina, Peters, David A., and Ormiston, Robert A., "Optimum Rotor Performance in Skewed Flow Based on Actuator-Disk Theory," Proceedings of the 27th AIAA Applied Aerodynamics

Conference, San Antonio, TX, June 22-25, 2009, AIAA- 2009-3517.

10. Hong, Sean, Peters, David A., and Ormiston, Robert A., “A Dynamic Inflow-Based Induced Power Model for General and Optimal Rotor Performance.”